University of Texas Rio Grande Valley

ScholarWorks @ UTRGV

5-1-1998

Radio pulse properties of the millisecond pulsar PSR J0437-4715. I. Observations at 20 centimeters

F. A. Jenet

S. B. Anderson

V. M. Kaspi

T. A. Prince

S. C. Unwin

Follow this and additional works at: https://scholarworks.utrgv.edu/pa_fac

Part of the Astrophysics and Astronomy Commons

Recommended Citation

RADIO PULSE PROPERTIES OF THE MILLISECOND PULSAR PSR J0437−4715. I. OBSERVATIONS AT 20 CENTIMETERS

F. A. JENET

California Institute of Technology, Space Radiation Laboratory, Pasadena, CA 91125; merlyn@srl.caltech.edu

S. B. ANDERSON

California Institute of Technology, Space Radiation Laboratory, Pasadena, CA 91125; sba@srl.caltech.edu

V. M. KASPI[1]

Department of Physics and Center for Space Research, Massachusetts Institute of Technology, 37-621, Cambridge, MA 02139; vicky@space.mit.edu

T. A. PRINCE

California Institute of Technology, Space Radiation Laboratory, Pasadena, CA 91125; prince@srl.caltech.edu

AND

S. C. UNWIN[2]

California Institute of Technology, Space Radiation Laboratory, Pasadena, CA 91125; scu@huey.jpl.nasa.gov

Received 1997 July 8; accepted 1997 December 12

ABSTRACT

We present a total of 48 minutes of observations of the nearby, bright millisecond pulsar PSR J0437−4715 taken at the Parkes Observatory in Australia. The data were obtained at a central radio frequency of 1380 MHz using a high-speed tape recorder that permitted coherent Nyquist sampling of 50 MHz of bandwidth in each of two polarizations. Using the high time resolution available from this voltage recording technique, we have studied a variety of single-pulse properties, many for the first time in a millisecond pulsar. We show that individual pulses are broad band, have pulse widths ranging from ~ 10 ($\sim 0°6$ in pulse longitude) to ~ 300 μs ($\sim 20°$) with a mean pulse width of ~ 65 μs ($\sim 4°$), exhibit a wide variety of morphologies, and can be highly linearly polarized. Single pulse peaks can be as high as 205 Jy (over ~ 40 times the average pulse peak), and have a probability distribution similar to those of slow-rotating pulsars. We observed no single pulse energy exceeding ~ 4.4 times the average pulse energy, ruling out "giant pulses" as have been seen for the Crab and PSR B1937+21 pulsars. PSR J0437−4715 does not exhibit classical microstructure or show any signs of a preferred timescale that could be associated with primary emitters; single pulse modulation has been observed to be consistent with amplitude-modulated noise down to timescales of 80 ns. We observe a significant inverse correlation between pulse peak and width. Thus, the average pulse profile produced by selecting for large pulse peaks is narrower than the standard average profile. We find no evidence for "diffractive" quantization effects in the individual pulse arrival times or amplitudes as have been reported for this pulsar at lower radio frequency using coarser time resolution. Overall, we find that the single-pulse properties of PSR J0437−4715 are similar to those of the common slow-rotating pulsars, even though this pulsar's magnetosphere and surface magnetic field are several orders of magnitude smaller than those of the general population. The pulsar radio emission mechanism must therefore be insensitive to these fundamental neutron star properties.

Subject headings: pulsars: individual (J0437−4715) — radio continuum: stars — stars: neutron

1. INTRODUCTION

Single-pulse studies of millisecond pulsars are considerably more difficult to perform than are those of slow pulsars. Faster data rates are needed to study millisecond pulsars with comparable pulse phase resolution, and finer radio frequency resolution is required to minimize the effect of interstellar dispersion. Also, interstellar scattering timescales comparable to the pulse duration render studying individual pulse morphologies impossible, while steep millisecond pulsar spectra preclude observations of sufficient sensitivity at higher radio frequencies where scattering is less important.

Yet single-pulse studies of millisecond pulsars are highly desirable for two reasons. First, the origin of the radio emis-

sion that has made isolated neutron stars famous is, even 30 yr after their discovery, still a mystery. The high brightness temperatures ($\sim 10^{30}$ K) associated with the radio emission point to coherent processes which are poorly understood even under less exotic conditions (Melrose 1996). Previous observations of slow pulsars have not sufficiently constrained the emission mechanism; the study of radio-emission properties of millisecond pulsars may provide important new clues. Millisecond pulsars, because of their fast spin periods, have much smaller light-cylinder radii, and hence magnetospheres, than slow pulsars. They also have lower surface magnetic field strengths than the general pulsar population (most likely resulting from their having been "recycled" by a binary companion through the accretion of mass and angular momentum). If the radio emission mechanism were at all dependent on such properties, millisecond pulsars should have different radio properties than the slower-spinning general population. The second reason single-pulse studies of millisecond pulsars are important is

---

[1] Hubble Fellow.
[2] Current address: Jet Propulsion Laboratory, Mail Stop 306-388, 4800 Oak Grove Drive, Pasadena, California 91109-8099.

that millisecond pulsar timing is well known to be an unparalleled source of precision astrometric and astrophysical information. Among factors possibly limiting timing precision is the stability of the average profile, which depends on the properties of single pulses.

Only recently has a systematic study of single pulses from millisecond pulsars become possible, largely due to improving computational and data recording technologies. To date, the only such investigation has been for the 1.5 ms pulsar PSR B1937A + 21 (Wolszczan, Cordes, & Stinebring 1984; Sallmen & Backer 1995; Backer 1995; Cognard et al. 1996). Interestingly, PSR B1937 + 21 exhibits giant radio pulses like those seen elsewhere only in the Crab pulsar. With the single-pulse properties of only one millisecond pulsar having been studied in any detail, the question of whether all millisecond pulsars show similar properties naturally arises. Unfortunately, PSR B1937 + 21 suffers interstellar scattering at timescales comparable to the duration of a single pulse at the radio frequencies at which it has been observed, rendering detailed study of individual pulse morphologies difficult.

Here we report on high time resolution single-pulse studies of a second millisecond pulsar, PSR J0437−4715. This pulsar's large flux density and low dispersion measure (DM), and the corresponding scarcity of line-of-sight scattering material, render it an obvious target for single-pulse work. Some single-pulse investigations of PSR J0437−4715 have been reported (Johnston et al. 1993; Ables et al. 1997) but none have had sufficient time resolution to resolve most individual pulses. By using a fast recording device and powerful supercomputers, we have been able to resolve all pulses in our data, the narrowest being ~ 10 μs.

2. OBSERVATIONS AND ANALYSIS

2.1. *Parkes Observations*

All data reported here were obtained at the 64 m radio telescope of Parkes Observatory in New South Wales, Australia on 1995 July 24 and 25 at a central radio frequency of 1380 MHz. Observations were made by using a cryogenically-cooled, dual-channel system which received orthogonal linear polarizations. The signal path from the receiver was as follows. A local oscillator signal, locked to the Parkes Observatory frequency standard, was amplified and then mixed with the incoming radio-frequency signal from the receiver and low-pass filtered to form a single-sideband intermediate frequency (IF). These IF signals (one for each polarization) were relayed to the control room, where they were amplified and mixed with a second local oscillator (LO). This second mixer operated as a baseband quadrature mixer, with the in-phase and quadrature-phase output signals low-pass filtered to 25 MHz. Thus, a total bandwidth of 50 MHz at center frequency 1380 MHz was available for recording. The four analog signals from the complex downconverter were then digitized with two-bit resolution and recorded at the Nyquist rate (400 Mbit s^{-1}) on a digital tape recorder (Datatape LP-400) along with timing information synchronized to the Parkes Observatory clock. The output bus operates at 50 Msample s^{-1} and is 8 bits wide: 2 digitizer bits × 2 polarizations × 2 signal phases. Thus, a single 13 minute observation resulted in 39 Gbytes of raw voltage data. Detailed information about the baseband mixing, digitizing, and data recording system is reported by Jenet et al. (1997).

The epochs and durations of the observations of PSR J0437−4715 reported on in this paper are summarized in Table 1. A calibration scan was done prior to observations 1 and 3 by moving the telescope off-source and pulsing a noise diode source at a fixed frequency. The amplitude of the calibration source and hence the absolute flux scale in janskys for our pulsar observations were determined by using observations of the bright radio continuum source Hydra.

2.2. *Data Analysis*

Storage of raw voltage data permits great flexibility in data analysis, but also requires significant computational power. Most data reduction was therefore done on the massively-parallel Caltech 512-node Intel Paragon XPS L38 supercomputer which has peak computation rate of 38.4 Gflop s^{-1}, as well as on the 32-node Intel Paragon XPS A4 supercomputer which has 4.3 Gflop s^{-1} peak computation rate. Data from the Datatape recorder were read into a 0.5 Gbyte Datatape variable rate buffer, and then onto the supercomputer file systems via a high-speed HIPPI network. Most analysis was done by using specialized parallel code written in C++, with the NX message passing interface. For details about the hardware and analysis software tools, see Jenet et al. (1997).

2.2.1. *Dedispersion*

Once on the parallel computers, the raw data are unpacked into floating point numbers and the interstellar dispersion is handled by one or both of two techniques. The first technique, and the less computationally intensive, uses a software "incoherent filter bank," which simulates the output of the conventional hardware filter-bank spectrometer, namely, samples of power in many individual narrow frequency channels. The channelized data are subsequently added with appropriate time delays to achieve a dedispersed time series that has time resolution limited by residual dispersion within channels. The second more computationally-demanding dedispersion method does a direct Fourier deconvolution of the interstellar medium transfer function, i.e., "coherent dedispersion" (Hankins & Rickett 1975). For PSR J0437−4715, it is easy to show that 128 filter-bank frequency channels are needed to minimize single-channel dispersion and time resolution. This results in a time resolution of 2.56 μs and a dispersion smearing of approximately 3.26 μs. In principle, coherent dedispersion can yield a time resolution equal to the inverse of twice the bandwidth; however, in practice, one is limited by the precision with which the DM is known. For PSR J0437−4715, the uncertainty on the published DM (Sandhu et al. 1997) implies that the true time resolution of our coherently dedispersed time series is no better than ~ 200 ns; we con-

TABLE 1

EPOCHS OF OUR PARKES 1380 MHz
OBSERVATIONS OF PSR
J0437 − 4715

Observation	MJD at start	Duration (minutes)
1	49922.81856	12.0
2	49922.82789	13.0
3	49923.84874	12.4
4	49923.85768	13.3

servatively chose to average our coherently dedispersed time series to a time resolution of 320 ns. Higher time resolutions, when necessary, were achieved by coherently dedispersing a smaller bandwidth, obtained by using a coarse-resolution software filter bank. For example, we achieved 80 ns resolution by coherently dedispersing a 6.25 MHz band. It is important to note that multifrequency DM measurements are very accurate, but not necessarily precise. Therefore, such DM values may be of limited use in single-pulse studies.

The presence of large amplitude signals in the two-bit quantized voltage data will introduce unwanted artifacts in the final dedispersed time series if proper care is not taken. For bright pulsars like PSR J0437−4715, appropriate corrections are crucial for proper pulse-morphology analyses. Two major quantization effects have been identified: (1) power underestimation and (2) power scattering. We have minimized the power underestimation effects at the data unpacking stage by dynamically adjusting the assigned voltage levels. The effects of the scattered power have only been corrected in the incoherently dedispersed data. A more detailed discussion of these quantization effects and the algorithms used to correct them may be found elsewhere (Jenet 1998).

Thus, we produced a (coherently or incoherently) dedispersed time series for each of the two polarizations. The mean value calculated over a megasample was then subtracted in each polarization, and a gain factor was applied to convert the raw data values to janskys. The channels were then added to yield the total intensity, or Stokes I. Faraday rotation in the interstellar medium causes a time delay between opposite circular polarizations, as well as a rotation of the angle of linear polarization across the band, however, given the low DM and rotation measure (Navarro et al. 1997), both effects are negligible here.

2.2.2. *Folding the Data with the Pulse Period*

The known pulsar ephemeris (Sandhu et al. 1997; provided for convenience in Table 2) was used with the TEMPO software package (Taylor & Weisberg 1989) to calculate the expected topocentric pulse period and the pulse phase once every 671 ms. The average pulse profile, shown in Figure 1,
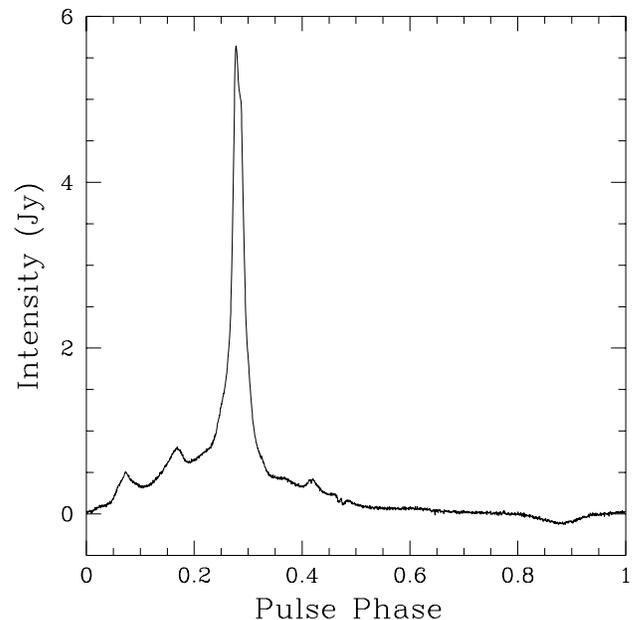

FIG. 1.—Average pulse profile obtained by folding data from observation 3 (see Table 1). There are 2048 bins across the pulse profile; dispersion smearing in the finite-width simulated filters is 3.26 μs, just larger than one bin. The small "dip" seen near phase 0.9 is an instrumental effect.

was obtained by dedispersing and folding the data in observation 3, assuming a DM of 2.64515 pc cm^{-3}. In the figure there are 2048 bins across the period, and the remaining dispersion smearing due to the finite size of the simulated filters is 3.26 μs, just larger than one bin. The pulse morphology is identical to that seen by other groups (e.g., Manchester & Johnston 1995; Navarro et al. 1997) except for the presence of a broad, shallow "dip" in the baseline. A spectral analysis shows that the dip is not dispersed. Hence, it is an instrumental artifact. Since each pulse of emission lasts only about 400 μs in our 50 MHz bandpass, the dip, which is about 2 ms away from the main peak, should not affect the remainder of the analysis. We suspect that this dip is the result of some nonlinear process occurring in the receiver chain when the pulse is outside of our bandpass, although we have not yet seen this effect in other pulsars observed with the same receiver chain.

3. RESULTS AND DISCUSSION

3.1. *General Features of Single Pulses*

Figure 2 is a gray-scale plot of 12.5 s of data phase aligned with the pulse peak. Only 368 μs on either side of the main peak is shown. Data used for this plot are incoherently dedispersed, corresponding to a time resolution of 2.56 μs with 3.26 μs DM smearing (as for Fig. 1). No evidence for drifting subpulses can be seen in this figure. Figure 2 does show regions where the pulse is absent, but we found that averaging as little as 10 of these regions reveals the presence of a pulse. Hence, we have no evidence for pulse nulling. The average fluctuation spectrum shown in Figure 3 displays a broad feature indicating a correlation or "memory" between pulses. The fluctuation spectrum is calculated by first extracting a time series of intensities at a fixed pulse phase and then Fourier transforming this time series (Backer 1973). In order to reduce the variance in the

TABLE 2

ASTROMETRIC AND SPIN PARAMETERS FOR PSR J0437 − 4715[a]

Parameter	Value
Right Ascension (J2000)	04^{h}37^{m}15^{s}748182(4)
Declination (J2000).......................	−47°15′08″23145(5)
$\mu_\alpha \cos \delta$ (mas y^{-1}).......................	121.34(6)
μ_δ (mas y^{-1})	−72.50(3)
Annual parallax (mas)	5.6(8)
Period, P (ms)	5.75745182525633(6)
Period derivative $\dot{P}$ (10^{-20})	5.7295(9)
Period epoch and position (MJD)......	50019.00
Dispersion Measure (cm^{-3} pc)	2.6469(1)
Binary period, P_b (d)....................	5.741042353935(350)
$x = a_p \sin i$ (lt-s).........................	3.36668528(4)
Eccentricity	0.00001920(2)
Longitude of periastron, ω (°)	1.793148(20000)
Periastron epoch (MJD).................	50000.49656856(40000)
$\dot{x}$ (10^{-12}lt − s s^{-1})	0.082(4)
Timing data span (MJD)	49373–50323

NOTE.—Units of right ascension are hours, minutes, and seconds, and units of declination are degrees, arcminutes, and arcseconds.
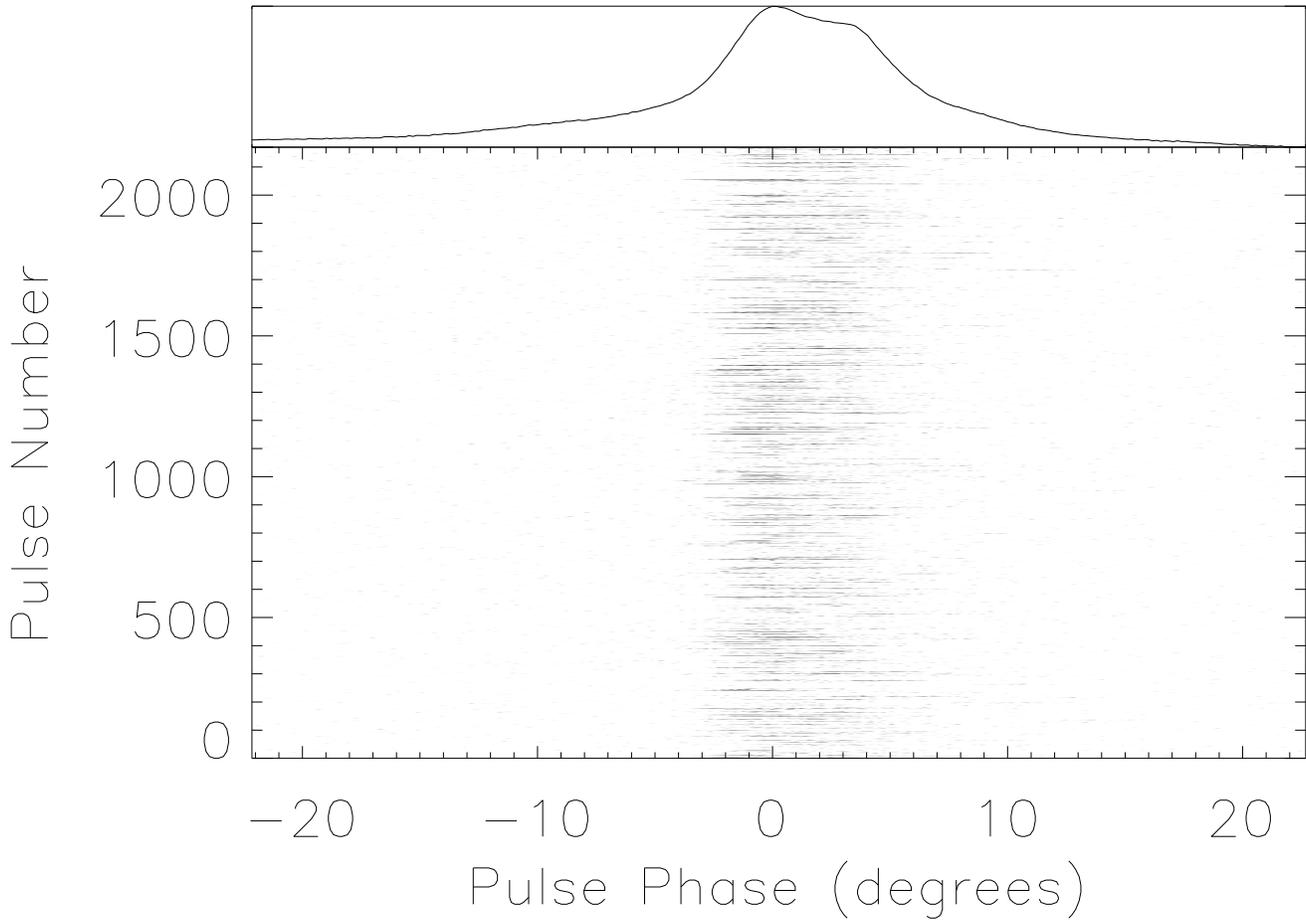
[a] Sandhu et al. 1997.

FIG. 2.—Gray-scale plot showing single pulses of PSR J0437−4715 during a single ∼13 s observation. Note that only the central ∼0.7 ms are shown; the average profile formed by these pulses is shown at the top.

spectrum, 392 consecutive 256 point spectra were averaged together. The fluctuation spectrum shown in Figure 3 was calculated at zero pulse phase. Structure in the fluctuation spectrum is common among slow pulsars (Manchester & Taylor 1977; Backer 1973). Figure 4 shows a "rogues gallery" of several phase-aligned subpulses from the same data set that produced Figure 2. It is clear from Figures 2 and 4 that, as is typical of pulsars, the average profile is a

sum of many individual subpulses, which, although forming a relatively stable average profile, individually exhibit a variety of morphologies.

Figure 5 shows a semilogarithmic histogram of subpulse peaks in units of janskys for observation 3.[3] Results for our other observations are similar. In observation 3 the mean pulse peak was 5.6 Jy. From Figure 5, the largest peaks in observation 3 were ∼40 times the mean value. We have included only subpulses that are statistically significant, i.e., the chances of randomly obtaining the measured on pulse power must have been less then one in 10^{11}, assuming Gaussian statistics.

The low flux-density cutoff therefore represents our sensitivity threshold, given the receiver noise temperature. Only 20% of pulses satisfied this criterion. The distribution for this 12.4 minute observation is well described over most of the observed pulse peak range by the expression

$$\log_{10}(N) = a + b \times P_{\text{peak}}, \tag{1}$$

where $a = 4.51 \pm 0.01$, $b = -0.0262 \pm 0.0002$ Jy^{-1}, P_{peak} is the peak power in janskys, and N is the number of pulses. However, extrapolating this expression to a pulse peak of 205 Jy suggests that only 0.14 pulses at this height should have been observed; the one that was seen at 205 Jy

FIG. 3.—Average intensity fluctuation spectrum calculated for 100,352 pulses at zero pulse phase (see text). The power density spectrum is normalized by the zero frequency power. The frequency axis is normalized by the pulsar frequency.

[3] The mean fluxes in the different observations were different because of scintillation. For simplicity we choose to report results from observation 3, in which the pulsar was brightest.
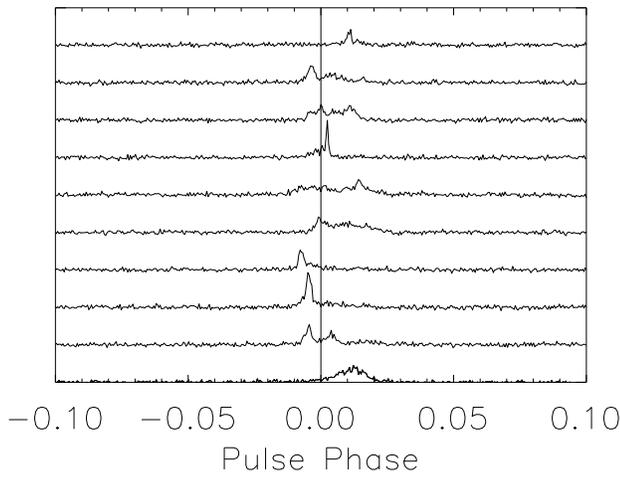
FIG. 4.—Random sampling of phase-aligned individual bright pulses from PSR J0437−4715, using a software filter bank. The time resolution in this plot is 2.56 μs, with 3.26 μs of DM smearing.
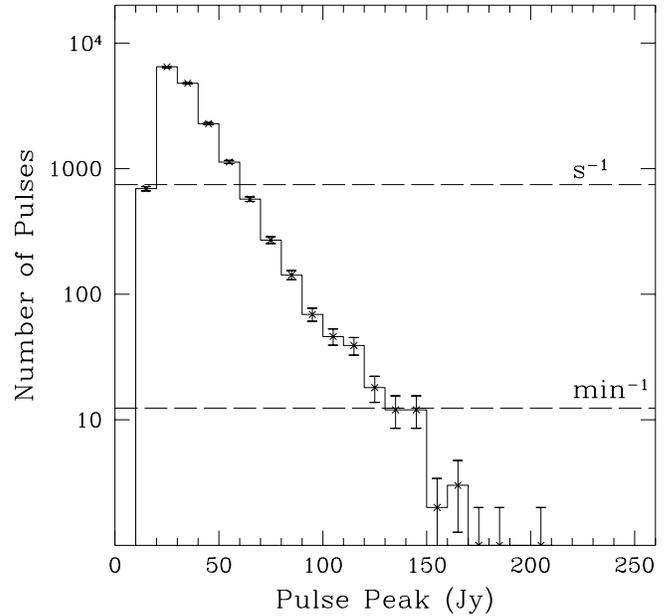
FIG. 5.—Histogram of peak pulse amplitudes in janskys from observation 3 (see Table 1), dedispersed using a software filter bank. The time resolution was 2.56 μs. Rates for two peak values (1 s^{-1} and 1 minute^{-1}) are indicated by dashed lines. The low flux-density cutoff is due to an imposed threshold criterion.

suggests that the distribution may have a high-peak tail that longer integrations might make observable.

Figure 6 shows a large amplitude subpulse coherently dedispersed with an intrinsic time resolution of 10 ns. Two factors limit our actual time resolution to ~ 200 ns: (1) DM uncertainties and (2) nonideal low pass filter response. The low pass filters used in the downconverter have a group delay of up to 80 ns at the upper band edge. Neither of these effects would hide the presence of a coherent signal:

although they would make a noise signal appear more like a Gaussian noise signal, they would not turn a coherent signal into a random noise signal. The envelopes superposed on the two linear polarizations represent the 98%
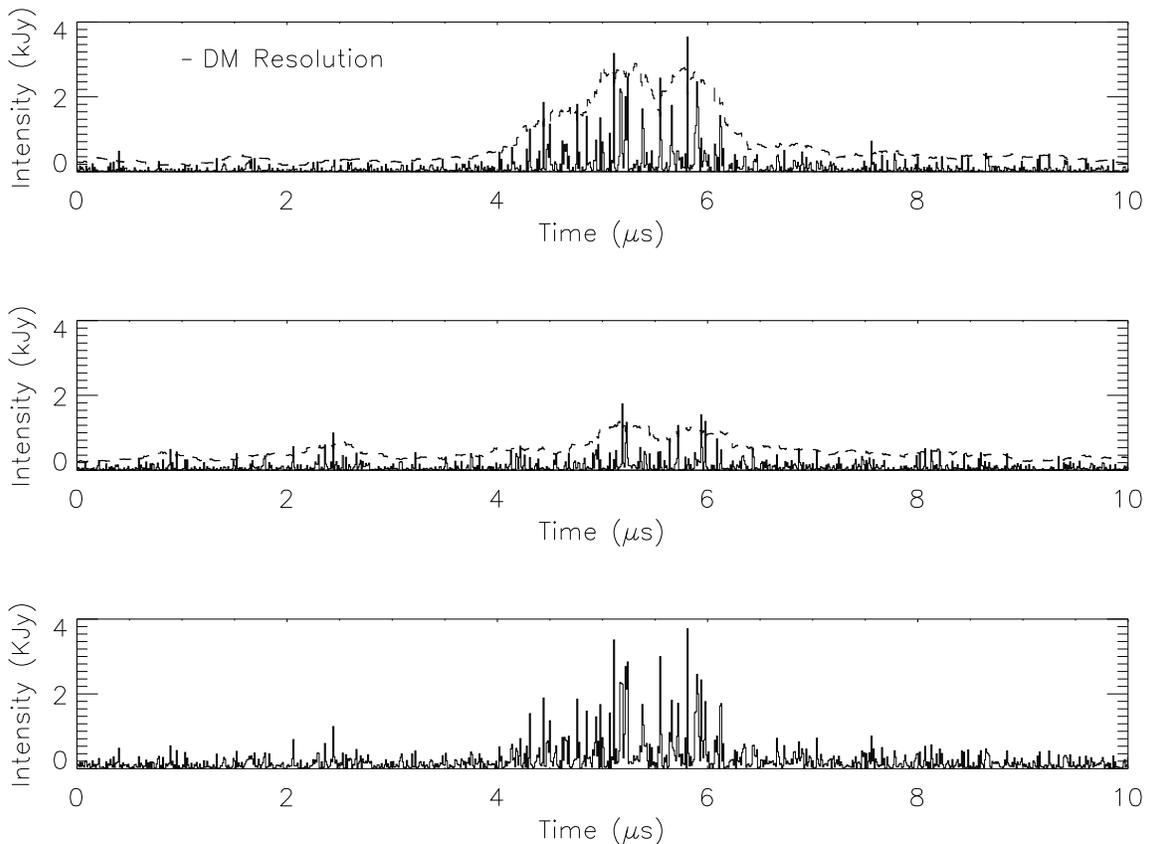
FIG. 6.—Largest amplitude pulse in our data. The time resolution is intrinsically 10 ns but is increased to 200 ns by DM uncertainties and nonideal filter response. The dashed line represents the 98% confidence level (see text).
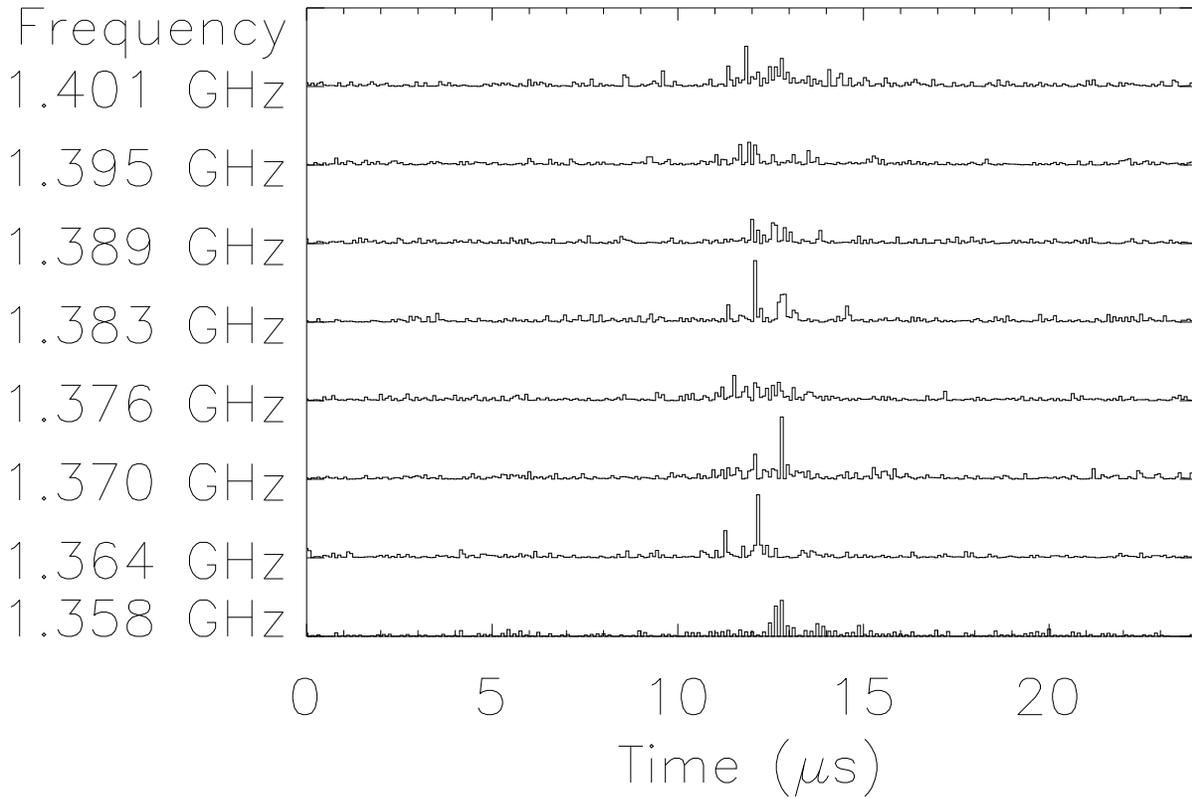
FIG. 7.—Largest amplitude pulse in our data, in each of eight frequency subbands. Here the data were coherently dedispersed, then subjected to an eight channel software filterbank at zero DM. The lowest frequency channel, the Nyquist channel, appears to have a lower signal-to-noise ratio because its statistics are intrinsically different from the other channels.

confidence levels for χ_1^2 statistics. If the statistics of the voltage data were given by a Gaussian distribution, we would expect the power to be given by a χ_1^2 distribution. Using 25 data points to either side of the point in question, we calculated the mean power and used it to find the value of the power such that the probability of being less then that value is 0.98. As can be seen from this figure, the statistics of the emission are consistent with modulated noise. It is also clear from Figure 6 that this single pulse is substantially linearly polarized. The largest 10 pulses in our data all show similar behavior.

The same subpulse is shown in Figure 7 in each of eight radio-frequency subbands. It is clear that this pulse is broad band, extending at least over 50 MHz bandwidth. The scintillation bandwidth at this frequency is much larger than 50 MHz, so it is not relevant. The subband structure is consistent with a Gaussian noise process.

"Giant pulses" from the millisecond pulsar PSR B1937+21 have been observed (Wolszczan, Cordes, & Stinebring 1984; Sallmen & Backer 1995; Backer 1995; Cognard et al. 1996), where "giant" implies single pulses having energies much larger than the average single-pulse energy. To investigate whether the large pulses seen in PSR J0437−4715 are also "giant" in this sense, we produced a histogram of pulse energies; this is shown in Figure 8 for observation 3. Results for the other observations are similar. Only statistically significant subpulses were included. The vertical dashed line indicates the mean energy. Its displacement at an energy lower than the peak of the distribution reflects the fact that the average pulse lies well below the noise. The figure demonstrates that there is no evidence for single pulses having energies larger than

~4.4 times the mean pulse energy. By contrast, if PSR J0437−4715 had the same pulse energy distribution as PSR B1937+21 in each of our 12 minute observations, we would have expected over 200 pulses to have energy greater than 5
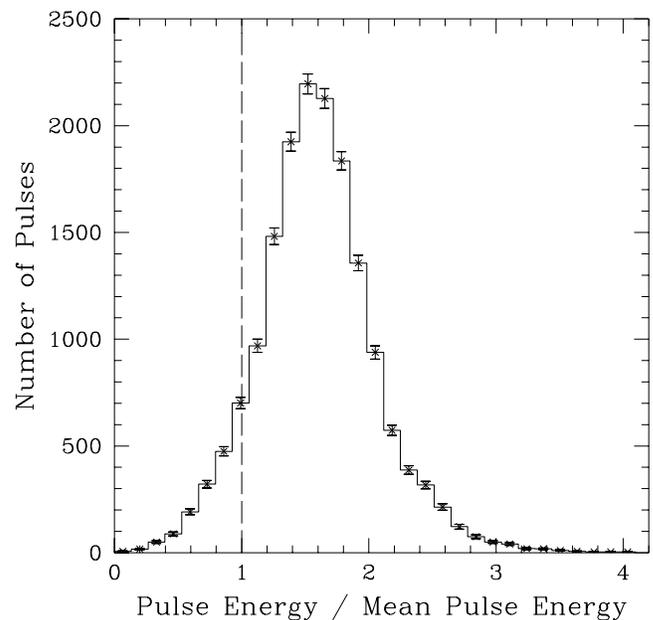

FIG. 8.—Histogram of pulse energies for observation 3, including only statistically significant pulses. The vertical dashed line is the mean pulse energy, which falls below the peak of the distribution, since the mean pulse is below the noise level. The largest pulse energy we observed was 4.4 times the mean.
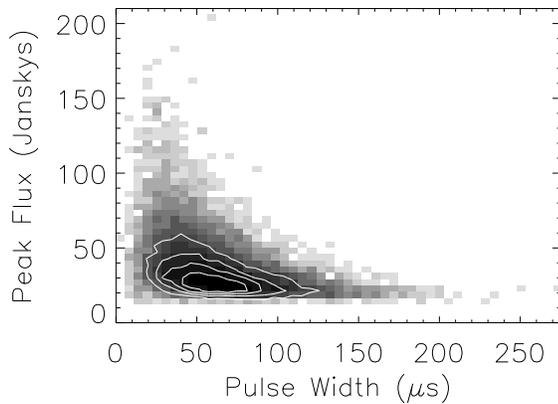
FIG. 9.—Pulse peak flux vs. pulse width. Only statistically significant pulses were included in this plot, hence the lower cutoff near the receiver noise temperature. Contours in the plot are 50, 100, 150, and 205 pulses.

times the mean. Thus, PSR J0437−4715 does not show any evidence for "giant pulses."

The narrow range of pulse energies exhibited in Figure 8, for a pulsar having very different single subpulse morphologies, suggests that there should be a correlation between pulse peak and width. This correlation is shown in Figure 9. In the plot only statistically significant pulses are included, which explains the lower cutoff in peak flux at the level of the receiver noise.

From Figure 9, it is clear that by selecting and folding only large amplitude pulses, one can obtain a "discriminated" average profile that is considerably narrower than the standard average profile. Figure 10 shows the average profile obtained by selecting the 500 single pulses which have the largest peak amplitudes in a ∼90 s span. Successively wider average profiles are obtained by lowering that threshold. The full width at half maximum (FWHM) of the discriminated average profile shown in Figure 10 is only ≃ 75 μs, which should be compared to the FWHM of the standard average profile, ≃ 145 μs. This is interesting, since timing precision improves as the average profile width decreases; thus, discriminated folding could, in principle, improve pulsar timing precision. However, at least in the case of PSR J0437−4715, the steep spectrum (Fig. 5, eq. [1]) of pulse amplitudes precludes timing resolution improvement.
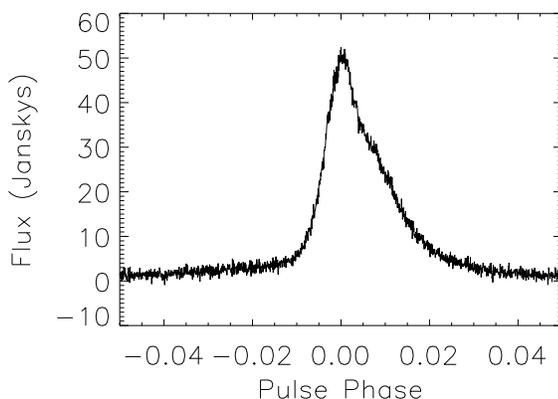
3.2. Search for Microstructure and Other Preferred Timescales

At least eight bright pulsars display structure in their emission on a timescale shorter than that of the widths of the average pulse profile and individual subpulses (Manchester & Taylor 1977). Such "microstructure" has not previously been detectable in millisecond pulsars because of both insufficient time resolution of observations and DM-smearing and multipath scattering. Our data on PSR J0437−4715 present the first opportunity to detect microstructure in a millisecond pulsar. Along with classical microstructure, we can also look for evidence of preferred timescales in the emission that may be due to the presence of primary emitters. The noiselike statistics of pulsar emission along with the high brightness temperatures lead one to postulate the existence of many coherent emitters, or primary emitters, adding up incoherently to form the observed emission (Melrose 1996).

We searched for preferred timescales by performing careful autocorrelation function (ACF) analyses of the incoherently and coherently dedispersed data. Preferred timescales would present themselves as rapid changes in the slope of the ACF (i.e., a "break") and/or local minima and maxima in the ACF. In the incoherently dedispersed data, the time resolution is limited to ∼3 μs; we find no evidence for microstructure in the ∼120,000 incoherently dedispersed pulses. In order to search with higher time resolution, ACFs were produced for ∼14,000 consecutive coherently-dedispersed pulses, as well as ∼1000 of the largest amplitude coherently dedispersed pulses. Note that the effective time resolution of the coherently dedispersed data is limited to ∼200 ns by DM uncertainties and nonideal filter response. No structure was seen in the ACF (See Fig. 11). It is possible that the microstructures could be individually narrow band. Hence, larger bandwidths may wash out any preferred timescales. We coherently dedispersed several subbands ranging in width from 6.25 to 781 KHz and centered at 1380 MHz. Again, we found no evidence for preferred timescales. Note that the highest time resolution achieved was 80 ns (= 1/2 × 6.25 × 10^6).

3.3. Coherent Radiation Patterns?

Ables et al. (1997) have reported on single-pulse observations of PSR J0437−4715 at an observing frequency of
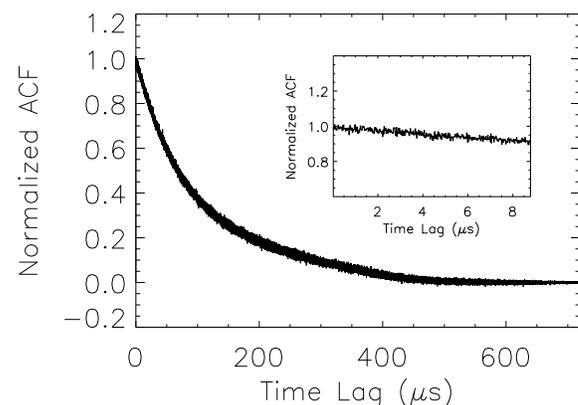

FIG. 10.—Average profile obtained by folding the 500 single pulses having the highest peak amplitudes in a ∼90 s data span. The width at half maximum here is 75 μs.

FIG. 11.—Autocorrelation function for ∼14,000 consecutive coherently dedispersed pulses. The inset is the same data plotted on a smaller scale. Since no sharp changes in the slope or local maxima or minima can be seen, there is no evidence for any preferred timescales other then the subpulse width.

326.5 MHz. They found regularly-spaced peaks in a smoothed arrival time distribution of the largest 500 single pulses in each of their 70 s samples. These peaks were spaced by ~ 20 μs, much less than their sample time, 102.4 μs. They argued, using simulations, that in spite of their relatively slow sampling, single-pulse arrival time uncertainties of ~ 5 μs could be obtained, and hence the fringes could be resolved. The fringes implied that certain pulse phases were preferred for single pulses, which they interpreted as evidence for a coherent diffractive radiation pattern in the pulsar's emission. They emphasized that their results were for the largest amplitude pulses only, which they assumed to be of different origin than the emission resulting in the standard profile. Their results predict that with higher time resolution observations, such as those discussed in this paper, the average profile obtained by folding the largest amplitude pulses should show the same fringe pattern.

Figure 10, in which we have folded only the highest amplitude pulses, shows no evidence for any structure, apart from an asymmetric shoulder on the leading edge, which was seen by Ables et al. (1997). We have repeated this analysis by varying the integration time and pulse threshold, and find similar results. We note that our fractional bandwidth is the same as that of Ables et al. (1997), hence the effects of the finite bandwidth should be identical. If their apparent fringes were due to a coherent diffractive radiation pattern, the fringe spacing should scale with wavelength; thus, we would have expected fringe spacings of ~ 4.7 μs, much larger than the 320 ns time resolution of Figure 10. Given the relative sensitivities of our observations and theirs together with the pulsar spectral index, we should have been able to observe their "spikes" with great ease. Thus, we find no evidence to suggest coherent radiation patterns exist.

It is possible to reconcile the disagreement by postulating that the "spikes" have a different radio spectrum than does the emission forming the average profile. Ultimately, high time resolution observations at 326.5 MHz will settle this issue.

4. CONCLUSIONS

We have presented the first detailed single-pulse study of a millisecond pulsar in which sufficient time resolution was available to resolve single pulses as they would be seen in the pulsar vicinity. The similarity of the single-pulse properties to those of normal slow pulsars is remarkable, given the dramatically reduced magnetospheric volume and magnetic-field strength of PSR J0437$-$4715. Indeed,

without being told the absolute sample rate, it is unlikely that one could distinguish between this being a millisecond or slow pulsar. To summarize, our observations of PSR J0437$-$4715 have:

1. resolved individual pulses, and shown that they have a wide variety of morphologies, with multiple subpulse components not uncommon,
2. shown that individual pulses are in general broad band,
3. shown that individual pulses can have high linear polarization,
4. provided neither evidence for giant pulses as observed in the Crab pulsar and PSR B1937$+$21 nor for pulse nulling or drifting subpulse phenomena,
5. found structure in the intensity fluctuation spectrum,
6. revealed a correlation of pulse peak with pulse width so that the average profile formed from only the highest amplitude pulses is much narrower than the conventional average profile,
7. not shown any evidence for microstructure or preferred timescales ≥ 80 ns,
8. shown that the emission is consistent with an amplitude modulated noise model,
9. provided no evidence to support the claim made by Ables et al. (1997) of the detection of coherent radiation patterns.

Because no self-consistent radio emission mechanism context exists (see, e.g., Melrose 1996) in which to discuss these results, it is difficult to say how such models are constrained. Indeed, previous slow pulsar single pulse studies suffered from the same difficulty. However, it is often the case that fundamental insights become apparent when known phenomenon are taken to extremes; this, and improved tape recording and computer technologies that permit single pulse studies of millisecond pulsars, provided our motivation in undertaking this analysis. Similar studies of other millisecond pulsars may eventually lead to an understanding of the radio emission mechanism.

REFERENCES

Ables, J. G., McConnell, D., Deshpande, A. A., & Vivekanand, M. 1997, ApJ, 475, L33
Backer, D. C. 1973, ApJ, 182, 245
———. 1995, A&A, 16, 165
Cognard, I., Shrauner, J. A., Taylor, J. H., & Thorsett, S. E. 1996, ApJ, 457, L81
Hankins, T. H., & Rickett, B. J. 1975, Methods Comput. Phys., 14, 55
Jenet, F. 1998, PASP, submitted
Jenet, F., Cooke, R., Prince, T. A., & Unwin, S. C. 1997, Publ. Astr. Soc. Pacific., 109, 707
Johnston, S., et al. 1993, Nature, 361, 613
Manchester, R. N., & Johnston, S. 1995, ApJ, 441, L65
Manchester, R. N., & Taylor, J. H. 1977, Pulsars (San Francisco: Freeman)

Melrose, D. B. 1996, in IAU Colloq. 160, Problems and Progress, ed. S. Johnston, M. A. Walker, & M. Bailes (San Francisco: ASP), 139
Navarro, J., Manchester, R. N., Sandhu, J. S., Kulkarni, S. R., & Bailes, M. 1997, ApJ, 486, 1019
Sallmen, S. & Backer, D. C. 1995, in ASP Conf. Ser. 72, Millisecond Pulsars: A Decade of Surprise, ed. A. S. Fruchter, M. Tavani, & D. C. Backer (San Francisco: ASP), 340
Sandhu, J. S., Bailes, M., Manchester, R. N., Navarro, J., Kulkarni, S. R., & Anderson, S. B. 1997, ApJ, 478, L95
Taylor, J. H., & Weisberg, J. M. 1989, ApJ, 345, 434
Wolszczan, A., Cordes, J. M., & Stinebring, D. R. 1984, in Millisecond Pulsars, ed. S. P. Reynolds & D. R. Stinebring (Green Bank: NRAO), 63